A theoretical insight into the photophysics of psoralen

Juan José Serrano-Pérez, Luis Serrano-Andrés,[a)] and Manuela Merchán
Instituto de Ciencia Molecular, Universitat de València, Doctor Moliner 50, Burjassot,
ES-46100 Valencia, Spain

Psoralen photophysics has been studied on quantum chemistry grounds using the multiconfigurational second-order perturbation method CASPT2. Absorption and emission spectra of the system have been rationalized by computing the energies and properties of the low-lying singlet and triplet excited states. The S_1 $\pi\pi^*$ state has been determined to be responsible of the lowest absorption and fluorescence bands and to initially carry the population in the photophysical processes related to the phototherapeutic properties of psoralen derivatives. The low-lying T_1 $\pi\pi^*$ state is, on the other hand, protagonist of the phosphorescence, and its prevalent role in the reactivity of psoralen is suggested to be related to the elongation of the pyrone ring C_3-C_4 bond, where the spin density is distributed on both carbon atoms. Analysis of energy gaps and spin-orbit coupling elements indicates that the efficient photophysical process leading to the population of the lowest triplet state does not take place at the Franck-Condon region but along the S_1 relaxation path. © 2006 American Institute of Physics. [DOI: 10.1063/1.2178794]

I. INTRODUCTION

Absorption of electromagnetic radiation by a chromophore triggers a chain of photochemical reactions which may be beneficially employed to treat some skin disorders and other diseases. Sometimes the chromophore is already present in the tissue and the phototherapy takes place naturally, e.g., the cure of neonatal hyperbilirubinemia or the photoregeneration of vitamin D.[1] However, in the treatment named photochemotherapy, a drug is administered to act as a photosensitizer, a substance which is harmless in the dark but active upon absorption of radiation, typically ultraviolet, visible, or near infrared light.[1] Two basic photochemical mechanisms are responsible for the phototherapeutical activity. The photosensitizer can directly react with DNA bases forming stable adducts which interfere the genetic activity.[1–5] On the other hand, the photosensitizer can transfer its excess energy to molecular oxygen available in the cellular environment, generating highly reactive singlet oxygen able to damage target tissues. This type of protocol is known as photodynamic therapy (PDT).[1,6,7]

A generally accepted classification of the photochemotherapeutic reactions comprises three types of mechanisms. Types I and II correspond to oxygen-dependent pathways for PDT activity, taking place when light, in the presence of a photosensitizer and molecular oxygen, induces a chemical reaction in a substrate.[1,6,8,9] In type I reactions, the photoactive compound in its triplet state promotes an electron transfer reaction to molecular oxygen, leading to the formation of $O_2\cdot$, $OH\cdot$, or $HO_2\cdot$ radicals. Type II reactions correspond to energy transfers from the triplet state of the photosensitizer to dioxygen, generating the reactive $^1\Delta_g$ excited state.[10] All these intermediate species later interact with components of the cell membrane leading to cellular damage that eventually contributes to skin photosensitization, mutation, error-prone DNA repair, and carcinogenesis.[1,8,11,12] In contrast to the previous mechanisms, oxygen-independent type III reactions lead to direct photobinding between the photosensitizer and the DNA base monomers.[13–15]

Furocoumarins (also named psoralens) are a class of heterocyclic compounds with a known phototherapeutic activity involving the three described mechanisms.[16] These systems have been found to possess mutagenic properties when applied in conjunction with near UV-A light (320–400 nm) exposure.[17,18] A specific treatment coined psoralen+UV-A (PUVA) therapy has been designed to treat different skin disorders such as psoriasis and vitiligo.[1,19,20] It is commonly assumed that the mechanism of PUVA therapy involves a [2+2]-photocycloaddition of psoralen in its lowest triplet state and a pyrimidine DNA base monomer that requires the transfer of hydrogen atoms or electrons without direct involvement of molecular oxygen. The photoreactive process seems to take place in three phases. The first step occurs in the dark: The furocoumarin is inserted between adjacent pyrimidine base pairs in the DNA duplex. In a second step, the absorption of one photon by psoralen induces the formation of monoadducts with the neighboring pyrimidine via interaction of the respective carbon-carbon double bonds that both compounds have. Two types of monoadducts, pyrone and furan types, can then be formed by interaction of the C–C double bond of the pyrimidine base with the C_3-C_4 double bond of the pyrone ring and the $C_4'-C_5'$ double bond of the furan ring in psoralens, respectively (see Fig. 1). In that regard, thymine has been established as the most favorable base to photoreact with furocoumarins, in accordance with its predominance in the formation of cyclobutane dimers (T<>T) in UV-irradiated DNA.[21,22] In a third step, the monoadduct may absorb another photon, inducing its other

a)Electronic mail: luis.serrano@uv.es

124, 124502-1
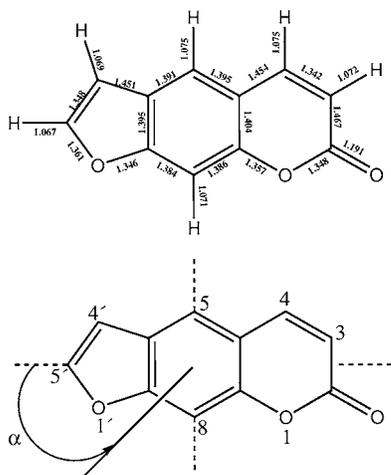
FIG. 1. Psoralen molecule atom labeling (bottom) and ground state optimized bond lengths in angstroms (top). The arrow defines the positive angles of both the dipole moment and electronic transition moment directions with respect to the pseudosymmetry long axis.

photoreactive C–C double bond to interact with a thymine on the opposite strand of DNA. Therefore, a diadduct that cross-links the DNA helix is formed.

The poly[dA-dT]·poly[dA-dT] sequence region seems to be the most favorable site for the photocycloaddition reactions of furocoumarins.[23] Several studies have suggested that, whereas the furan monoadduct forms a diadduct, the pyrone monoadduct does not.[3,5,24] Formation of cross-links was thought to be extremely relevant for the therapeutic effectiveness, although it is also known that the diadduct causes adverse side effects such as carcinogenesis, mutagenesis, and immunosuppression difficult to repair.[3,8] Only furocoumarins with bifunctional groups such as psoralen can form diadducts and may produce undesired lethal and mutagenic consequences. Certain monofunctional furocoumarins have been proved to yield as efficient phototherapy as bifunctional furocoumarins, suggesting that the induction of lesions in DNA cannot be considered as the only mechanism responsible for the phototherapeutic effects[5] and most probably a PDT process also takes place. The detailed characterization of the mechanisms is still under intense research.

Understanding the photophysical properties of furocoumarins represents a crucial step in order to rationalize the corresponding phototherapeutic mechanisms. The low-lying region of the absorption spectrum of psoralen, the reference compound, has two main bands: A weak and structured band is observed ranging from 360 to 270 nm (3.44–4.77 eV) and a sharp feature appears at 240 nm (5.16 eV) in aqueous solution and ethanol.[25,26] Both fluorescence and phosphorescence emissions have been detected for psoralen in ethanol (77 K) at 409 nm (3.03 eV) and 456 nm (2.72 eV, T_0), respectively. The phosphorescence/fluorescence quantum yield ratio, 7.1, indicates the effectiveness of an intersystem crossing (ISC) mechanism.[27] It has been proposed that photoreactivity of furocoumarins proceeds through the triplet state in all types of photosensitization, that is, PDT and PUVA therapies.[5] It can be therefore expected that increasing of the triplet formation quantum yield leads to an enhancement of the phototherapeutic action.

From the photochemical standpoint, an effective photosensitizer should possess, in principle, certain desirable key features: it must be harmless in the dark; in order to treat deep tissues, it should be activated by long wavelength light, because the longer wavelength radiation the photosensitizer absorbs, the deeper the energy penetrates in the body; its triplet state must be efficiently populated from the excited singlet state and effective in transferring the energy to molecular oxygen in the PDT mechanism; and finally, it should form monoadducts and perhaps not diadducts with DNA to avoid mutagenic side effects. Additionally, a good photosensitizer should be amphiphilic to favor the injected administration of the drug, easily synthesized or isolated from natural sources, be deactivated soon after the treatment, and quickly eliminated from the body.[1]

We are currently undertaken a project to study, using quantum-chemical methods, the photophysics and photochemistry of furocoumarins and related compounds in order to rationalize the basic features responsible of their phototherapeutic properties. In the present paper we start by considering the photophysical properties of parent psoralen (7-H-furo[3,2-g][1]-benzopyran-2-one, see Fig. 1). The low-lying excited states of the molecule have been computed within the framework of multiconfigurational second-order perturbation theory, in particular, with the CASPT2 method. Absorption, fluorescence, and phosphorescence spectra have been characterized, together with other spectroscopic parameters required to understand the photophysics of the compound: related oscillator strengths, dipole moments, emission radiative lifetimes, and spin-orbit couplings. Knowledge on theoretical grounds about these properties in psoralen shall hopefully guide future research on the photochemical mechanisms of phototherapeutical activity of furocoumarins and derivatives. In the light of the present results, previous experimental[23,25–28] and theoretical[13,29–32] findings shall also be considered.

II. COMPUTATIONAL DETAILS

Using the CASSCF multiconfigurational wave functions as reference, the second-order perturbation theory through the CASPT2 method was employed to include dynamic correlation energy in the calculation of the electronic excited states. The CASPT2 method calculates the first-order wave function and the energy up to second order and has repeatedly proved its accuracy.[33–37] The imaginary level-shift technique was employed in order to prevent the effect of intruder states. A shift parameter of 0.3 a.u. was selected by checking the stability in the excitation energies.[38,39] The molecular symmetry was constrained to the C_s point group. For geometry optimizations, however, relaxing the symmetry constraints had no effect on the final structure, which preferred in all cases to maintain planarity. An atomic natural orbital (ANO-L)-type basis set contracted to C,O[4s3p1d]/H[2s1p] (Refs. 40 and 41) was used throughout except in the calculation of the lowest-lying Rydberg state, for which the basis set was enlarged with an additional s diffuse function placed in the charge centroid of the cation and built as re-

ported elsewhere.[35,42] The carbon and oxygen $1s$ core electrons were kept frozen in the second-order perturbation step.

Geometries were obtained by computing analytical gradients at the RASSCF level of calculation for the ground and the lowest singlet and triplet excited states. In the optimization of the A' states an active space of 14 active orbitals and 16 electrons has been employed and up to quadruple excitations were considered (eight orbitals in RAS1 space and six orbitals in RAS3 space). Within the irreducible representations (a', a'') of the C_s group this active space can be labeled as (0,14). An additional oxygen lone-pair orbital was included in the active space (1,14) in order to optimize the lowest A'' excited states. In all the remaining calculations, CASSCF wave functions were generated as state-average (SA) CASSCF roots of a given symmetry. Based on preliminary RASSCF calculations, the CASSCF active space was reduced to include 12 active electrons and 12 active orbitals (RAS2 0,12) for A' roots and 14 active electrons and 13 active orbitals (RAS2 1,12) for A'' roots. The number of selected SA-CASSCF roots were 11, 4, 7, and 3 for $^1A'$, $^1A''$, $^3A'$, and $^3A''$ symmetries, respectively. The CAS state interaction method[43] (CASSI) was used to compute transition properties, including the spin-orbit coupling (SOC) elements between selected states as described elsewhere.[44] All calculations in the present paper were performed with the MOLCAS-6.0 quantum chemistry software.[45,46]

III. RESULTS AND DISCUSSION

A. Absorption spectrum

Our final goal is to understand the photophysical properties of psoralen in order to relate the obtained information to its biological activity. We first start by studying the singlet-singlet and singlet-triplet spectra of the molecule. Several singlet excited states have been computed vertically at the S_0 ($1\,^1A'$) ground state optimized RASSCF structure. The results are compiled in Table I. Hereafter only CASPT2 results will be discussed. The lowest singlet excited state, $2\,^1A'(\pi\pi^*)$, lies vertically at 3.98 eV with a related oscillator strength of 0.027. Next, the $1\,^1A''(n\pi^*)$ state is found at 5.01 eV corresponding to a transition predicted with negligible intensity. A third transition to the $3\,^1A'$ state has been computed at 5.03 eV with an oscillator strength of 0.107. Unlike the other $\pi\pi^*$ states, the $3\,^1A'$ state has a high dipole moment, 8.72 D, differing by more than 2.5 D from that of the ground state, an indication of its sensitivity to polar environments, in which the related transition is expected to undergo a redshift. The recorded absorption spectra in different solvents, from cyclohexane[47] to water,[26] displays a weak and structured band ranging from 360 to 270 nm (3.44–4.77 eV). Depending on the band resolution and the environment, one or two maxima near 330 and 280 nm (3.76 and 4.43 eV, respectively) have been described. The present computed results suggest that this set of features can be better assigned just to the $2\,^1A'(\pi\pi^*)$ transition, with the weak $n\pi^*$ band lying beneath. In that case, the observed band profile should be attributed to vibrational structure. This is not unlikely, considering that a noticeable rearrangement of the bond distances of the molecule occurs at the $2\,^1A'$ minimum.

TABLE I. Computed excitation energies ΔE (eV), oscillator strengths f, dipole moments μ (D), and dipole moment, μ_{dir} (deg), and transition dipole moment, TDM$_{dir}$ (deg), directions for the low-lying electronic transitions of psoralen.

State	ΔE_{CASSCF}	ΔE_{CASPT2}	f	μ	μ_{dir}	TDM$_{dir}$
$1\,^1A'$	⋯	⋯		6.25	128	⋯
$2\,^1A'(\pi\pi^*)$	4.52	3.98	0.027	6.50	132	4
$1\,^1A''(n\pi^*)$	4.22	5.01	0.000	2.07	130	⋯
$3\,^1A'(\pi\pi^*)$	6.33	5.03	0.107	8.72	132	5
$4\,^1A'(\pi\pi^*)$	6.68	5.22	0.064	7.07	−23	−10
$5\,^1A'(\pi\pi^*)$	6.73	5.30	0.331	7.07	−37	102
$6\,^1A'(\pi\pi^*)$	6.95	5.70	0.091	7.37	−37	30
$7\,^1A'(\pi\pi^*)$	7.21	5.81	0.321	6.58	−34	127
$8\,^1A'(\pi\pi^*)$	7.30	6.17	0.287	6.56	−42	4
$9\,^1A'(\pi\pi^*)$	7.57	6.24	0.168	4.25	−35	−7
$10\,^1A'(\pi\pi^*)$	7.72	6.28	0.012	6.29	−40	−7
$2\,^1A''(n\pi^*)$	6.39	6.32	0.000	0.11	43	⋯
$1\,^3A'(\pi\pi^*)$	2.57	3.27	⋯	5.40	124	⋯
$2\,^3A'(\pi\pi^*)$	3.13	3.55	⋯	5.35	125	⋯
$3\,^3A'(\pi\pi^*)$	3.82	4.08	⋯	5.48	127	⋯
$4\,^3A'(\pi\pi^*)$	4.18	4.66	⋯	5.97	129	⋯
$5\,^3A'(\pi\pi^*)$	4.43	4.67	⋯	5.41	124	⋯
$6\,^3A'(\pi\pi^*)$	5.68	4.84	⋯	6.78	−31	⋯
$1\,^3A''(n\pi^*)$	4.07	4.85	⋯	2.15	111	⋯

Furthermore, the structure of the band disappears in different media and also in all psoralen derivatives, even in selenopyrane and thyopyrane psoralen derivatives.[26] Calculations at the time-dependent density-functional theory[13,48] (TD-DFT) and DFT/multireference configuration interaction[32] (MRCI) levels of theory suggest, however, that two $\pi\pi^*$-type transitions computed near 3.8 and 4.4 eV are really responsible of the low-energy band. A definitive assignment would require a full analysis of the vibrational structure of the band and comparison with spectra in the vapor or in molecular beams.

Above 5.0 eV several singlet-singlet transitions have also been computed. Transitions to the $4\,^1A'$ (5.22 eV) and $5\,^1A'$ (5.30 eV) ($\pi\pi^*$) excited states have oscillator strengths of 0.064 and 0.331, respectively. The recorded spectra show a single and sharp band peaking near 248 nm (5.00 eV) in cyclohexane[47] and 240 nm (5.16 eV) in ethanol and water.[25,26] In principle, the observed feature can be assigned to transition to the $3\,^1A'$ state at 5.03 eV. Moreover, taking into account our computed results, an additional band with higher intensity can be expected at higher energies (5.30 eV). The measured band is probably a combination of both transitions. Between 5.7 and 6.2 eV four medium to intense transitions to $^1A'$ $\pi\pi^*$ excited states are predicted. Above this energy only weak transitions of valence $\pi\pi^*$ and $n\pi^*$ character have been obtained up to 8.0 eV. The beginning of the Rydberg series has been determined at 6.32 eV, as the $2\,^1A''$ [highest occupied molecular orbital (HOMO) $\rightarrow 3s$] state. Two intense bands peaking at 210 nm (5.90 eV) and 200 nm (6.20 eV) have been reported for psoralen in 1,1,1,3,3,3-hexafluoro-2-propanol.[47] They clearly correspond to the transitions to our computed $7\,^1A'$ and $8\,^1A'$ $\pi\pi^*$ states, representing the most intense bands in that energy region of the spectrum. Song *et al.*[25] reported that the two lowest-energy absorption bands in psoralen, angelicin, and

$1\,^1A'$ (gs) → $2\,^1A'$ ($\pi\pi^*$) $1\,^1A'$ (gs) → $1\,^1A''$ ($n\pi^*$)

$1\,^1A'$ (gs) → $1\,^3A'$ ($\pi\pi^*$) $1\,^1A'$ (gs) → $1\,^3A''$ ($n\pi^*$)

FIG. 2. Differential electron density for the main valence transitions in psoralen computed at the ground state optimized geometry. The electron density is shifted upon light-induced excitation from darker to lighter regions.

methylpsoralens are polarized along the long axis and nearly parallel, with angles differing less than 20°. Transition dipole moment (TDM) directions indicate that the three lowest $\pi\pi^*$ features have nearly parallel polarizations, that is, they are aligned with the long axis of the molecule, while transition to the $5\,^1A'$ state has essentially perpendicular polarization.

Regarding the vertical excitations to the triplet states, the $1\,^3A'$ $\pi\pi^*$ (T_1) state lies at 3.27 eV, near 0.7 eV below the $2\,^1A'$ (S_1) state. Three other $^3A'$ $\pi\pi^*$ states are next in energy at 3.55, 4.08, and 4.66 eV. The lowest triplet state of $n\pi^*$ character, $^3A''$, has been located vertically at 4.85 eV, slightly below with respect to its corresponding singlet state. TD-DFT (Ref. [13]) and DFT/MRCI (Ref. [32]) results obtained similar results for the location of the triplet states, although, as it is typical for DFT-based methods,[49] singlet-triplet transitions are underestimated (0.2–0.3 eV).

The nature of the low-lying transitions of each symmetry, which are those basically responsible for the photophysical properties of psoralen, can be graphically described by computing the differential electron density plots as displayed in Fig. 2. Transition to the S_1 $\pi\pi^*$ state is mainly benzene-like, with the charge migration concentrated in the central benzenoid ring. On the contrary, that related to the T_1 $\pi\pi^*$ state has its major contributions in the pyrone ring, with high participation of the carbonyl oxygen and a shift in the density away from the pyrone ring C_3–C_4 bond, which will be later discussed as an essential feature of the photophysics of the system. Also in Fig. 2, we find the expected differential density plots of the $n\pi^*$ states focused on the carbonyl group.

B. Emission spectra

Fluorescence has been reported for psoralen in polar solvents starting (T_0) at 350 nm (3.54 eV) with a maximum at 409 nm (3.03 eV).[27,28] Phosphorescence has also been recorded in solution with band origin at 456 nm (2.72 eV) and a maximum between 460 and 490 nm (2.7–2.5 eV). Psoralens are characterized by a weak fluorescence emission and strong phosphorescence bands. In particular, in psoralen, the fluorescence quantum yield was measured in ethanol, Φ_F =0.019 (Refs. [27]) and 0.02,[28] while the phosphorescence

TABLE II. Computed and experimental energy differences (eV) and emission radiative lifetimes (τ_{rad}) relevant for the photophysics of psoralen. E_{VA}: vertical absorption, T_e: adiabatic electronic band origin, E_{VE}: vertical emission, Abs_{max}: experimental absorption maximum, T_0: experimental band origin, and E_{max}: emission maximum.

State	Theoretical (CASPT2)				Experimental[a]			
	E_{VA}	T_e	E_{VE}	τ_{rad}	Abs_{max}	T_0	E_{max}	τ_{rad}
$2\,^1A'(\pi\pi^*)$	3.98	3.59	3.45	74 ns	3.7–4.3	3.54	3.03	⋯
$1\,^1A''(n\pi^*)$	5.01	3.91	2.78	3 μs	⋯	⋯	⋯	⋯
$1\,^3A'(\pi\pi^*)$	3.27	2.76	2.29	28 s	⋯	2.7	2.7	5–8 s
$1\,^3A''(n\pi^*)$	4.85	3.84	2.79	9 ms	⋯	⋯	⋯	⋯

[a]Data in ethanol (Refs. 25–28 and 55). See also other solvents (Ref. 47).

quantum yield was reported to be $\Phi_P=0.13$.[27] The obtained ratio Φ_P/Φ_F is approximately 7.1. The total phosphorescence decay time (τ_P) has been established in glycerol-water as 1.1 s (Ref. [28]) and in ethanol as 0.66 s.[27] The phosphorescence radiative lifetime can be therefore obtained as τ_{rad} ($=\tau_P\Phi_P$) from 8 to 5 s.

Our computed results on Table II allow the rationalization of part of the experimental data. The low-lying singlet excited $2\,^1A'(\pi\pi^*)$ state is responsible for the lowest-energy absorption and emission fluorescence bands. Vertically, at the ground state geometry, the transition energy is computed to be 3.98 eV and, upon relaxation of the geometry, the band origin (T_e) obtained as the energy difference between the ground and the excited state minima decreases to 3.59 eV. A similar relaxation is observed experimentally between the lowest-energy reported absorption band maximum and the band origin. The computed changes in the optimal geometries between the ground (S_0) and the $2\,^1A'(\pi\pi^*)$ (S_1) states affect the bond alternation of the system, mainly in the central ring (cf. Figs. 1 and 3), as expected from the discussion on the differential charge density plots of Fig. 2. By using the Strickler-Berg relationship,[36,50,51] a fluorescence radiative lifetime of 74 ns is calculated for the S_1 state. The low-lying

FIG. 3. Psoralen molecule optimized bond lengths (Å) in different electronic singlet states. Top: $2\,^1A'(S_1, \pi\pi^*)$; bottom: $1\,^1A''(S_2, n\pi^*)$.

FIG. 4. Psoralen molecule optimized bond lengths (Å) in different electronic triplet states. Top: $1\,{}^3A'(T_1,\pi\pi^*)$; bottom: $1\,{}^3A''(T_7,n\pi^*)$.

FIG. 5. Spin density for the low-lying triplet states in psoralen computed at the ground state optimized geometry.

$1\,{}^1A''(n\pi^*)$ state (vertically S_2) is shown to relax its energy by more than 1 eV upon geometry optimization. The main variations are obtained in the pyrone ring (up to -0.13 Å) and in the $C={O}$ bond length (0.16 Å). Although the $1\,{}^1A''(n\pi^*)$ minimum belongs to the S_1 hypersurface, the final T_e value is near 0.3 eV higher in energy than the computed and measured band origin for $2\,{}^1A'(\pi\pi^*)$. Therefore the $n\pi^*$ state it is not a plausible candidate for the fluorescence, which is better attributed to the $\pi\pi^*$ state. To support the assignment we cannot rely on the dependence of the recorded fluorescence emission on the solvent polarity, which is not clear in psoralen. Nevertheless, it is possible to support the assignment by comparing intrinsic fluorescence lifetimes. In principle, no experimental lifetimes have been reported, but from our computed radiative lifetimes, 74 ns for $2\,{}^1A'(\pi\pi^*)$ and 3 μs for $1\,{}^1A''(n\pi^*)$, and the experimental fluorescence quantum yield (0.016),[27] they can be deduced as 1.2 and 72 ns, respectively. Taking into account that the reported measurements were performed at time resolutions not lower than 2 ns,[27] the lack of measured lifetimes points out to a preferred assignment to the $(\pi\pi^*)$ S_1 state, with a faster fluorescence decay. Certainly, studies at a higher time resolution would be desirable.

The $1\,{}^3A'(\pi\pi^*)$ state is clearly protagonist of the phosphorescence. A band origin computed at 2.76 eV perfectly relates to the observed value in solution at 2.72 eV.[27] The change in geometry calculated from the ground state minimum is here more pronounced, in particular, at the pyrone ring, while the relaxation in energy reaches nearly 0.5 eV (cf. Fig. 4). The largest structural change is computed for the C_3-C_4 bond of the pyrone ring, which enlarges upon absorption and further relaxation by near 0.13 Å. The computed spin population, displayed in Fig. 5, is mainly placed on each of the carbon atoms forming the bond. In that way, psoralen becomes highly reactive in its lowest triplet state through its pyrone C_3-C_4 bond. This finding is the cornerstone of the photophysics of psoralen, which has been repeatedly pro-

posed to take place through a reactive triplet state, and it is also in agreement with the structure proposed for the phosphorescence band, mainly based on the intense vibrational progression corresponding to a $C={C}$ stretching mode in the pyrone moiety.[27] The computed phosphorescence radiative lifetime is 28 s, slightly higher than those estimated experimentally from the quantum yield and the total relaxation time, 5 and 8 s.[27,28] For the $2\,{}^3A'(\pi\pi^*)$ state the spin population is placed mainly on the carbon atoms forming both $C={C}$ bonds, that is, C_3-C_4 (pyrone) and $C_4'-C_5'$ (furan).
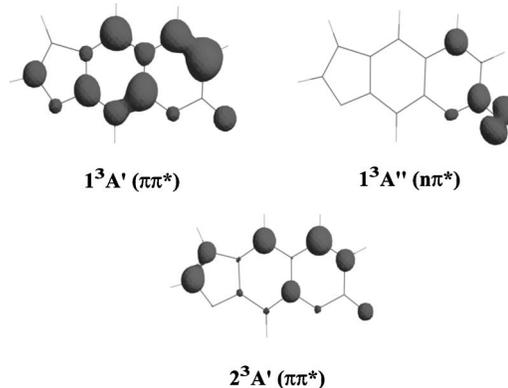
C. Photophysics of psoralen

Since the phototherapeutic properties of psoralen initiate by irradiation with light of wavelengths of 320–400 nm (3.87–3.10 eV), the only state which will be significantly populated by direct absorption is the spectroscopic $2\,{}^1A'(\pi\pi^*)S_1$ singlet state. The excited molecule will evolve towards the minimum of S_1, from which fluorescence will take place. The recorded phosphorescence/fluorescence emission ratio of 7.1 (Ref. 27) emphasizes the role of the triplet states in the photophysics of the system. That is, the lowest-lying triplet $1\,{}^3A'(\pi\pi^*)T_1$ must be populated, either by direct absorption or by means of an effective intersystem crossing mechanism. T_1 state lies much lower in energy than the S_1 state, both vertically (≈ 0.6 eV) and adiabatically (≈ 1.2 eV). The occurrence of direct interaction between both vertical states is unlikely, and therefore another mechanism has to be found, involving probably population of higher-lying triplet states continued by internal conversions towards T_1. In order to populate a triplet state by direct absorption, the spin-orbit coupling between the initial ground state and any of the low-lying triplet states should be quite large. The qualitative El-Sayed rules[52] indicate that the spin-orbit coupling is maximum between states of $\pi\pi^*$ and $n\pi^*$ types and minimum between states of the same nature. The spin-orbit matrix element between the ground S_0 and the low-lying $1\,{}^3A''(n\pi^*)$ state is computed to be 47 cm^{-1}, a large value that leads to a small combined oscillator strength of 5×10^{-6} for the corresponding spin-forbidden transition. The high phosphorescence quantum yield requires, however, a much more efficient procedure to populate T_1, and therefore an intersystem crossing (ISC) must be involved in the

photophysics. There are two necessary conditions for an effective ISC to take place: low energy gap and high spin-orbit coupling between a singlet and a triplet state. If the initially populated state is $2\,^1A'(\pi\pi^*)S_1$, the nonradiative decay to a triplet state must occur along the relaxation pathway of S_1, starting from the Franck-Condon region (ground state geometry), and in close vicinities of a singlet-triplet crossing. Analyzing the vertical energy differences between the S_1 and the triplet states, the gaps are quite large, while the spin-orbit coupling (SOC) elements are small. For instance, the largest SOC, 3 cm^{-1}, occurs between $2\,^1A'(\pi\pi^*)$, that is, S_1, and $1\,^3A''(n\pi^*)$, vertically T_7, which are separated by 0.87 eV. A similar value of 10 cm^{-1} was obtained at the DFT/MRCI level.[32] Other gaps and couplings studied at the Franck-Condon region are of minor importance. In order to fully understand the intersystem crossing mechanism responsible for the population of the reactive T_1 state in psoralen, the relaxation pathways of the energy should be computed, searching for regions with near degeneracies or crossings between the S_1 and triplet states having also large SOCs. These studies are the object of our future research.

IV. SUMMARY AND CONCLUSIONS

In the present research the photophysics of psoralen has been studied using quantum-chemical methods through the multiconfigurational second-order perturbation procedure CASPT2, employing high-quality ANO-type one-electron basis sets. Optimized geometries for the low-lying singlet and triplet states, energy differences, and state and transition properties provide us with important information to understand the excited state structure and the absorption and emission processes taking place upon irradiation of the molecule. The absorption spectrum of the system has been studied by computing vertical excitation energies. A low-lying S_1 singlet excited state of $\pi\pi^*$ character with a benzenelike nature is shown to lie at the energies in which the molecule is irradiated in phototherapy. This state is also proven to be responsible of the recorded fluorescence in different media by computing the emission properties and comparing them to the experimental measurements. Regarding the triplet state structure, a $T_1\,(\pi\pi^*)$ state is computed at low energies as responsible for the strong phosphorescence of the system. Analysis of the energy gaps and spin-orbit couplings at the Franck-Condon region suggests that the process responsible for the population of T_1 does not take place vertically and most probably it occurs along the relaxation path on the S_1 hypersurface. The study of the proper regions for favorable intersystem crossing requires the calculation of minimum energy paths and singlet-triplet crossings. On the other hand, the suggested role of the $S_2\,(n\pi^*)$-type state in the mechanism,[27] based on the assumption of the traditional proximity effect[53] between singlet $\pi\pi^*$ and $n\pi^*$ states, is unlikely. This type of reasoning is always based on vertical gaps, while modern photophysics is based in most of the cases on nonadiabatic processes along the energy relaxation paths.[36,44,54] Finally, the reactivity of psoralen in its T_1 state and the suggested role of such state in phototherapy are rationalized in terms of the computed spin density distributed on the two carbon atoms of the pyrone ring C_3-C_4 bond, which varies from a double- to a single-type character.

[1] R. Bonnett, *Chemical Aspects of Photodynamic Therapy* (Gordon and Breach Science, Amsterdam, 2000).
[2] B. R. Scott, M. A. Pathak, and G. R. Mohn, Mutat Res. **39**, 29 (1976).
[3] P. S. Song and K. J. Tapley, Jr., Photochem. Photobiol. **29**, 1177 (1979).
[4] E. Ben-Hur and P.-S. Song, Adv. Radiat. Biol. **11**, 131 (1984).
[5] D. Averbeck, Photochem. Photobiol. **50**, 859 (1989).
[6] R. Bonnett, Chem. Soc. Rev. **24**, 19 (1995).
[7] A. M. Rouhi, Chem. Eng. News **76**, 22 (1998).
[8] P. C. Joshi and M. A. Pathak, Biochem. Biophys. Res. Commun. **112**, 638 (1983).
[9] Y. N. Konan, R. Gurny, and E. Allémann, J. Photochem. Photobiol., B **66**, 89 (2001).
[10] S. Wang, R. Gao, F. Zhou, and M. Selke, J. Mater. Chem. **14**, 487 (2004).
[11] N. J. De Mol and M. J. Beijersbergen van Henegouwen, Photochem. Photobiol. **33**, 815 (1981).
[12] H. Meffert, F. Böhm, and E. Bauer, Stud. Biophys. **94**, 41 (1983).
[13] J. Llano, J. Raber, and L. A. Eriksson, J. Photochem. Photobiol., A **154**, 235 (2003).
[14] J. Cadet and P. Vigny, in *Bioorganic Photochemistry*, edited by H. Morrison (Wiley, New York, 1990), Vol. 1.
[15] C. M. Estévez, A. M. Grana, M. A. Ríos, and J. Rodríguez, J. Mol. Struct.: THEOCHEM **77**, 163 (1991).
[16] F. Dall'Acqua and P. Martelli, J. Photochem. Photobiol., B **8**, 235 (1991).
[17] W. L. Fowlks, J. Invest. Dermatol. **32**, 249 (1959).
[18] M. A. Pathak and J. H. Fellman, Nature (London) **185**, 382 (1960).
[19] A. B. Lerner, C. R. Denton, and T. B. Fitzpatrick, J. Invest. Dermatol. **20**, 299 (1953).
[20] J. A. Parrish, T. B. Fitzpatrick, L. Tannenbaum, and M. A. Pathak, N. Engl. J. Med. **291**, 1207 (1974).
[21] M. Aida, M. Kaneko, and M. Dupuis, in *Computational Molecular Biology*, edited by J. Leszczynski (Elsevier, Amsterdam, 1999), Vol. 8.
[22] B. Durbeej and L. A. Eriksson, Photochem. Photobiol. **78**, 159 (2003).
[23] D. J. Yoo, H. D. Park, A. R. Kim, Y. S. Rho, and S. C. Shim, Bull. Korean Chem. Soc. **23**, 1315 (2002).
[24] L. Musajo and G. Rodighiero, in *Photobiology*, edited by A. G. Giese (Academic, New York, 1972), Vol. 7.
[25] P.-S. Song, S. C. Shim, and W. W. Mantulin, Bull. Chem. Soc. Jpn. **54**, 315 (1981).
[26] M. Collet, M. Hoebeke, J. Piette, A. Jakobs, L. Lindqvist, and A. Van de Vorst, J. Photochem. Photobiol., B **35**, 221 (1996).
[27] W. W. Mantulin and P. S. Song, J. Am. Chem. Soc. **95**, 5122 (1973).
[28] E. Yeargers and L. Augenstein, J. Invest. Dermatol. **44**, 181 (1965).
[29] E. Yeargers and L. Augenstein, Nature (London) **212**, 251 (1966).
[30] G. G. Aloisi, F. Elisei, S. Moro, G. Miolo, and F. Dall'Acqua, Photochem. Photobiol. **71**, 506 (2000).
[31] N. E. Koval'skaya and I. V. Sokolova, High Energy Chem. **36**, 193 (2001).
[32] J. Tatchen, M. Kleinschmidt, and C. M. Marian, J. Photochem. Photobiol., A **167**, 201 (2004).
[33] K. Andersson, P.-Å. Malmqvist, and B. O. Roos, J. Chem. Phys. **96**, 1218 (1992).
[34] L. Serrano-Andrés, M. Merchán, I. Nebot-Gil, R. Lindh, and B. O. Roos, J. Chem. Phys. **98**, 3151 (1993).
[35] B. O. Roos, K. Andersson, M. P. Fülscher, P.-Å. Malmqvist, L. Serrano-Andrés, K. Pierloot, and M. Merchán, in *New Methods in Computational Quantum Mechanics*, Advances in Chemical Physics, Vol. XCIII, edited by I. Prigogine and S. A. Rice (Wiley, New York, 1996), pp. 219–331.
[36] L. Serrano-Andrés and M. Merchán, in *Encyclopedia of Computational Chemistry*, edited by P. v. R. Schlegel *et al.* (Wiley, Chichester, 2004).
[37] M. Merchán and L. Serrano-Andrés, in *Computational Photochemistry*, edited by P. v. R. Schleyer, P. R. Schreiner, H. F. Schaefer III, W. L.

Jorgensen, W. Thiel, and R. C. Glen (Elsevier, Amsterdam, 2005).

[38] B. O. Roos, K. Andersson, M. P. Fülscher, L. Serrano-Andrés, K. Pierloot, M. Merchán, and V. Molina, J. Mol. Struct.: THEOCHEM **388**, 257 (1996).

[39] N. Forsberg and P.-Å. Malmqvist, Chem. Phys. Lett. **274**, 196 (1997).

[40] J. Almlöf and P. R. Taylor, J. Chem. Phys. **86**, 4070 (1987).

[41] P.-O. Widmark, P.-Å. Malmqvist, and B. O. Roos, Theor. Chim. Acta **77**, 291 (1990).

[42] L. Serrano-Andrés, R. Lindh, B. O. Roos, and M. Merchán, J. Phys. Chem. **97**, 9360 (1993).

[43] P. Å. Malmqvist and B. O. Roos, Chem. Phys. Lett. **155**, 189 (1989).

[44] M. Merchán, L. Serrano-Andrés, M. A. Robb, and L. Blancafort, J. Am. Chem. Soc. **127**, 1820 (2004).

[45] K. Andersson, M. Barysz, A. Bernhardsson *et al.*, MOLCAS, Version 6.0, Department of Theoretical Chemistry, Chemical Center, University of Lund, P.O.B. 124, S-221 00 Lund, Sweden 2002.

[46] V. Veryazov, P.-O. Widmark, L. Serrano-Andrés, R. Lindh, and B. O. Roos, Int. J. Quantum Chem. **100**, 626 (2004).

[47] H. Matsumoto and Y. Ohkura, Chem. Pharm. Bull. (Tokyo) **11**, 3433 (1978).

[48] A. Nakata, T. Baba, H. Takahashi, and H. Nakai, J. Comput. Chem. **25**, 179 (2003).

[49] D. J. Tozer, R. D. Amos, N. C. Handy, B. O. Roos, and L. Serrano-Andrés, Mol. Phys. **97**, 859 (1999).

[50] J. L. McHale, *Molecular Spectroscopy* (Prentice-Hall, Upper Saddle River, NJ, 1999).

[51] Ò. Rubio-Pons, L. Serrano-Andrés, and M. Merchán, J. Phys. Chem. A **105**, 9664 (2001).

[52] P. Avouris, W. M. Gelbart, and M. A. El-Sayed, Chem. Rev. (Washington, D.C.) **77**, 793 (1977).

[53] W. A. Wassam, Jr. and E. C. Lim, J. Chem. Phys. **68**, 433 (1978).

[54] M. Merchán and L. Serrano-Andrés, J. Am. Chem. Soc. **125**, 8108 (2003).

[55] T. A. Moore, M. L. Harter, and P.-S. Song, J. Mol. Spectrosc. **40**, 144 (1971).